WOOD RESEARCH
64 (3): 2019
373-388

PREDICTION THE FATIGUE LIFE OF WOOD-BASED PANELS

Sergiy Kulman, Liudmyla Boiko
Zhytomyr National Agroecological University
Faculty of Forestry
Department of Wood Processing
Zhytomyr, Ukraine

Diana Hamáry Gurová, Ján Sedliačik
Technical University in Zvolen
Faculty of Wood Sciences and Technology
Department of Furniture and Wood Products
Zvolen, Slovak Republic

ABSTRACT

This work presents the results of an experimental investigation of the vibration response of cyclically loaded wood-based panels. The maximum temperature of the stationary state of the activation zone of samples of wood-based panels in the form of a rigid cantilever with their cyclic load at loading frequencies from 0 to 50 Hz and maximum internal stresses from 0.98 to 5.36 MPa was investigated. The purpose of this study is to determine the temperature of self-heating and to determine the dependence of the temperature on the loading conditions. The mathematical model is proposed in the form of system nonlinear ordinary differential equations, where stress, strain and temperature were used as the essential variables. The behaviour of the system is completely determined by the ratio of the introduced external energy and the value of the order parameter. The critical value of the order parameter depends on the thermo-physical properties of the material and is equal to the ratio of the value of the heat transfer coefficient multiplied by the area of thermal dispersion to the coefficient of linear thermal expansion.

KEYWORDS: Wood-based composites, fatigue life prediction, nonlinear dynamic, self-heating effect, thermo-elastic stress analysis.

INTRODUCTION

Polymer composite materials (PCM) which also includes wood and wood-based composite materials are widely used in many areas of technology due to their valuable properties (Ihnát et al. 2017). They have high ratio of the tensile strength of the material to its density. In many

cases, these materials are used in structures that are subjected to cyclic or vibration loads. A feature of the behaviour of PCM under the action of cyclic loads is their self-heating due to the nature of their physical properties. Their large nonlinearity in response to external thermo-moisture-force effects their low thermal conductivity. Self-heating of components from PCM and the achievement by them of some maximum permissible value of the self-heating temperature leads to their premature destruction. Therefore, it is necessary to understand this behaviour and to develop appropriate methods and models for diagnostics and monitoring purposes. The study of long durability of wood-based boards allows revealing the nonlinear nature of the reactions of these materials at power and temperature actions (Kulman and Boiko 2016, Kulman et al. 2017, Iždinský and Reinprecht 2017, Deliiski et al. 2019).

Nonlinearity at the same time is manifested in the absence of directly proportional reciprocal reactions to these actions (Boiko et al. 2013). This leads to the impossibility of applying the principle of superposition during their quantitative modelling, and for each nonlinear system, it is necessary to search their methods of research and description. Identifying possible research paths allows computational experiment. Understanding the nonlinearity of the behaviour of solids during loading is associated with the ideas of qualitative analysis of dynamic systems. The dynamics of the destruction of wood-based composites was considered in the conditions of prolonged exposure to constant load (Kúdela 2017). In these conditions, there is an increase of local temperature in the areas of over stresses, and in the role of the thermostat for the local areas of overstress, it is the deformed body itself (Kulman 2014, Kulman and Boiko 2016).

However, the temperature of the system may vary both under the influence of external conditions (heating or cooling), and under the influence of internal factors caused by the release or absorption of heat as a result of deformation. The deformation model must take into account the fact that the inner temperature of deformable body becomes a function of time, and there is necessary to take into account its energy balance in the conditions of the changing temperature. Since fatigue fracture has a thermal activation, a change in temperature causes a change in the rate of destruction. The Arrhenius Eq. 1 often expresses this dependence:

$$k = k_0 e^{\frac{-E_a}{RT}} \tag{1}$$

where: E_a – the activation energy (J·mol^{-1}),
k_0 – pre-exponential multiplier having a constant of velocity.

Taking into account that the deformation change depends not only on the change in the stresses but also on the temperature change, the Hooke's law is represented as the Duhamel-Neumann equations with only one coordinate (Landau and Lifshitz 1986):

$$\varepsilon_x = \varepsilon_{\sigma_x} + \varepsilon_{T_x} = \frac{1}{E}(\sigma_x - \nu(\sigma_y + \sigma_z)) + \alpha(T - T_0) \tag{2}$$

Solving the Eq. 2 with a respect to σ_x, and excluding, for simplification, the consideration of the Poisson effect; is obtained:

$$\sigma_x = E\varepsilon_x + \alpha(T - T_0)E \tag{3}$$

Eq. 3 takes into account the amount of stresses from external stresses (surface forces) and internal volumetric forces associated with the thermal expansion of the body.

The elastic loading causes not only reversible changes in the size and shape of the body, but also the change in the characteristics of the internal atomic-molecular dynamics. Here, the thermoelastic effect (Joule's effect) is shown – change in the temperature of elastic bodies that have an adiabatic load. With a single-load, the temperature change ΔT of the body, which is at a temperature T, is determined by the Kelvin formula (Thomson 1853):

$$\Delta T = -\frac{\alpha T}{C}\sigma \tag{4}$$

where: σ – uniaxial tension, positive during stretching and negative during compression,
α – coefficient of linear thermal expansion along the load axis,
C – heat capacity unit of body volume.

The Joule effect and Thomson's formula were the basis for new approaches to analysing the stress-strain state of solids under stress. These methods of analysis, called thermoelastic stress analysis, are developing rapidly in recent years (Lin and Rowlands 1995, Dulieu-Barton and Stanley 1999, Palumbo et al. 2017, Sfarra et al. 2017, Paynter and Dutton 2003, Jones and Molent 2004, Emery and Dulieu-Barton 2010, Fruehmann et al. 2010, Uenoya and Fujii 2000, Yoshida et al. 2012).

Thermoelasticity is one of the main causes of the self-heating effect during cyclic deformation of polymers. Many studies have been devoted to this effect (Naderi and Khonsari 2012, Toubal et al. 2006, Katunin 2017, Novák et al. 2017, Pavlinec et al. 2018). At the same time, many factors are controversial in terms of their explanations, and many phenomena have not been fully studied and explained. For example, what factors depend on and how is determined the value of the average temperature of the activation zone in the steady state. What is the transition mechanism (how does the transition occur) from the stationary state of the system to the non-stationary state? However, as a rule, in the construction of the behaviour model of the materials under study under the assumption, it is assumed that the material behaves adiabatically. However, such an assumption is not justified in all cases.

When one-piece, elastic loaded specific work, and therefore, increase in the specific internal energy of the body approximate (without taking into account the Poisson effect) is:

$$\Delta W(\sigma) = \int_0^{\sigma} \sigma(\varepsilon) d\varepsilon \tag{5}$$

ε - is a relatively elastic deformation of the body.

The change in the value of the specific thermal energy of the body during loading follows from Eq. 4:

$$\Delta Q(\sigma) = C\Delta T = -\alpha T\sigma \tag{6}$$

The study of the dynamics of interaction between temperature and internal stresses during deformation and destruction of composite materials on the basis of wood showed (Kulman 2015) that it is precisely the lagging of the change in the local temperature in the zone of destruction from the change in local internal stress in this zone, leads to periodic production of entropy, and eventually to destruction.

The purpose of this study is to identify and determine the conditions for the occurrence of the stationary state of the system and determine which factors affect its stability. The aim

of this study is creation a dynamic model of the process of deformation-destruction of wood-based composite materials under the action of cyclic loading and to carry out its computational and experimental verification.

MATERIAL AND METHODS

Material

Commercially-produced structural particleboard of urea-formaldehyde resin (UF) bonded boards were provided by Kronospan UA Ltd., particleboard type P2 according to EN 312; EN 13501-1: class D-s1, d0. One regular-size (2750 × 1830 mm) panel with the thickness of 10 mm was cut into 600 × 50 mm pieces. Before testing, panels were conditioned at 20°C and moisture content of 65%. Specimens were preheated in the chamber until they reached equilibrium with the target temperature. Mechanical properties of prepared samples were tested according to ASTM D 1037-12 at the target temperature, (Tab. 1).

Tab. 1: Constant factors and characteristics of the material.

Characteristics of the material Particleboard – type P2	
Thickness, (mm)	10 ± 0.1
Modulus of rupture, MOR (MPa)	20 ± 0.2
Modulus of elasticity, MOE (MPa)	2600 ± 20
Density, ρ (kg·m^{-3})	750 ± 7
Coefficient of thermal expansion, α (m·K^{-1})	0.00006
Heat transfer coefficient, h (W·m^{-2} K^{-1})	6
Specific heat, C_p (J·kg^{-1}K^{-1})	2300
Length activation volume, L (m)[a]	0.050
Activation volume width, B (m)[a]	0.016
Thickness of activation volume, (m)[a]	0.003
Activation volume, V_a (m^3)	2.2E-06
The length of the heat transfer section, (m)	0.050
The width of the heat transfer section, (m)	0.022
Heat transfer area, S_a (m^2)[a]	0.0022

[a]V_a, S_a – determined by measuring the actual thermal field during testing.

Testing of samples was carried out on a console bended with rigid fastening frequencies f = 8.3 Hz; 16.7 Hz; 25.0 Hz; 33.3 Hz; 41.7 Hz; 50.0 Hz. Twenty samples were tested at each frequency to obtain statistically significant results. Length of the consoles L = 220; 240; 260; 280; 300; 400; 500 mm. Amplitude of oscillation A = 12.5 mm. The temperature of 298 K and moisture content 65% were constant throughout all series of tests. The scheme and photograph is presented in Fig. 1.

The experimental test bench contains a frame 1 with a rigid holder 2 where the test sample 3 is fixed. In order to reduce heat loss in the activation zone, heat-insulating gaskets 4 are installed between the holder 2 and sample 3. The actuator 5 contains a crank-rocker mechanism 6 connected to the free end of the console 3. The temperature in the activation zone is measured by an infrared camera 7 and recorded in computer 8.

Measurement of the temperature of the region of maximum stresses (in the area of fixing the console) was carried out continuously throughout the test up to destruction. As a measuring device, an infrared camera (FLIR i3) was used. The accuracy of the temperature measurement is $\Delta T = \pm 0.1$ K.

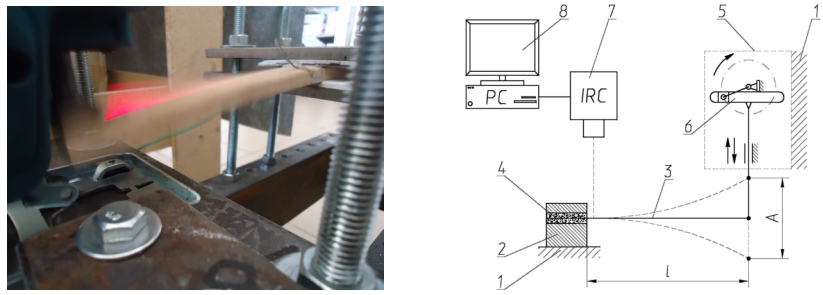

Fig. 1: Experimental stand and scheme.

Methods

The mathematical model of dynamic behaviour PCM in the form of thermoelastic oscillator (TEO) was created based on the law of conservation of energy. The inflow of energy from the external environment was denoted in the form of the thermal energy of the thermostat and the cyclic mechanical force, which causes deformation of the elastic body and creates internal stresses through $Q^{+}(T)$.

The outflow of energy to the external medium was denoted from the TEO side by heat transfer, without dividing it into convective, radiation, and others through $Q^{-}(T)$. The change in the internal energy of the TEO in time under the action of the external thermomechanical load is denoted as the difference in inflow and outflow of energy in the system:

$$\rho C_p \frac{dT(t)}{dt} = Q^{+}(T) - Q^{-}(T), \qquad Q^{+}(T) = Q_1^{+}(T) + Q_2^{+}(T) \tag{7}$$

$$Q_1^{+}(T) = V_A f \varepsilon \sigma 2, \quad Q_2^{+}(T) = \alpha (T - T_0)\, f V_A \sigma, \quad Q^{-}(T) = hS (T - T_0) \tag{8}$$

where: ρ - the density (kg·m^{-3}),
C_p - specific heat capacity (J·kg^{-1}·K^{-1}),
$Q_1^{+}(T)$ - thermal effect during periodic compression of the body due to the thermoelastic effect in the course of cyclic loading,
J; $Q_2^{+}(T)$ - thermal equivalents of deformation,
J; α - the coefficient of linear temperature expansion,
K^{-1}; h - coefficient of heat transfer (W·m^{-2}·K^{-1}),
S_a - heat transfer area (m^2),
V_A - activation volume of the sample (m^3),
f - cyclic load frequency (Hz),
T_0 - the temperature of the thermostat at the time $t = 0$, (K).

A dynamic model describing the evolution of TEO in time during cyclic loading is given in the form of a system of differential Eq. 9 that takes into account the mutual influence of temperature, stress and strain in the thermo-activation zone (Kulman 2015):

$$\begin{cases} \dfrac{dT(t)}{dt} = V_A f \dfrac{1}{2\rho C_\rho}\sigma\varepsilon - \alpha f (T - T_0)\sigma V_A \dfrac{1}{\rho C_\rho} - hS\dfrac{1}{\rho C_\rho}(T - T_0) \\ \dfrac{d\sigma(t)}{dt} = \varepsilon E + \alpha(T - T_0)E - (\sigma + Y) \\ \dfrac{d\varepsilon(t)}{dt} = \alpha(T - T_0) - \dfrac{\sigma + Y}{E} \\ \dfrac{dY(t)}{dt} = M\sin(x) \\ \dfrac{dx(t)}{dt} = \delta \end{cases} \tag{9}$$

where: T_0 - thermostat temperature (K),
E - modulus of elasticity (MPa),
α - coefficient of linear expansion (K^{-1}),
$\sigma(t),\varepsilon(t),T(t)$ - current values of stress, strain and temperature,
Y - stress from external cyclic load (MPa),
M - amplitude of oscillations (MPa),
f - frequency of oscillations (s^{-1}),
x - internal time of the system (introduced for solving a system of differential equations of computational methods);
t - time (s),
δ - constant (in the first approximation, it is assumed to be 1).

$T(t),\varepsilon(t),\sigma(t)$ – temperature, strain and stress are the phase variables of the state vector of the system q(T,ε,σ), which describes the behaviour of the system at different time intervals at different levels of its states and determines the dimension of the phase space equal to three; α, V_A, ρ, C_ρ, h, S, γ, $T0$, E, M, f, δ – are control (managing) parameters, constants, on the values of which the behaviour of phase variables depends. Their number is fixed and imposed on the system from the outside – the control parameters do not change as the system changes. The attention is focused on those situations where behaviour of the system changes qualitatively when the control parameters change. If the structure is preserved when the environmental conditions change, that is, control parameters, then this structure is called stable or structurally stable. But if the structure changes, there is relative instability. Synergetic focuses its attention on qualitative changes in those instabilities that are caused by a change in management parameters. Under the new control parameter, the system itself creates specific structures, which is called self-organization (Haken 1983).

First, the stationary state of the Eq. 9 is studied. The stationary state of the system is determined by its attractor. It is obvious that in the stationary state the system will be located only if the first time derivative of the temperature equals zero, i.e. in steady state, $dT/dt = 0$; $d\sigma/dt = 0$; $d\varepsilon/dt = 0$. Proceeding from this condition, the Eq. 9 was analysed and get:

$$\sigma_s = \frac{hS}{\alpha f V_A} \tag{10}$$

$$T_s = T_0 \frac{\alpha f V_A Y - hS}{\alpha^2 f V_A E} \tag{11}$$

σ_s, T_s - average stress and temperature in the activation zone in the stationary state of the system.

From Eq. 10 follows that the steady state can be written:

$$\sigma_s f V_A = \frac{hS}{\alpha} \tag{12}$$

Where the left side of Eq. 12 is the flow of external mechanical energy into the system in the amount $Q^+ = \sigma_s f V_A \left[\frac{n}{m^2} s^{-1} m^3 = \frac{nm}{s} = \frac{J}{s} = W \right]$, whereas the right side of this equation expresses the outflow in the form of thermal energy from the system due to heat transfer:

$$Q^- = \frac{hS}{\alpha} \left[\frac{Wm^2}{m^2 K K^{-1}} = W \right]$$

Thus, the stationary state of the system is characterized by equality of the inflow and outflow of energy from the activation volume: $Q^+ = Q^-$. Therefore, the dimensionless parameter equal to their ratio will be the criterion of the system stationarity:

$$K_S = \frac{Q^-}{Q^+} \tag{13}$$

and will describe the behaviour of the system near its steady state. When $Ks < 1$, the system will be in an asymptotically unstable state, since the inflow of external energy is greater than the outflow of energy from the system due to heat transfer. When $Ks > 1$, the system will be in an asymptotically stable state, since the inflow of external energy is less than the outflow of energy from the system due to heat transfer. If, on the basis of the stationary conditions in the left part, parameters related to the conditions of external influence on the system were selected and the geometric parameters of the system itself, then only the thermo-physical constants will remain in the right part (which are assumed to be constant in the first approximation). Thus, a criterion equal to h/α which limits the left side of Eq. 12 is obtained and this allows to assign their optimal values. Eq. 12 relates the quantitative ratios of the critical parameters of the external load to the thermo-physical characteristics of the material by the coefficient of heat transfer and the coefficient of linear expansion, which allows to find the critical value of one of the parameters for the external load at a known value of the other.

RESULTS AND DISCUSSION

Experiment in-situ

The experimental factors levels and test results are shown in Tab. 2. For identical samples and identical conditions of their fixation depending on the magnitude of the external load, which is determined by the frequency of oscillations and stresses, the average temperature of the sample in the steady state Ts will be different. Under the influence of an external cyclic load, the temperature in the activation zone gradually increases to a certain value and then stabilizes. This suggests that an open system gradually moves from an equilibrium state to a stationary state, which is characterized by an average temperature Ts. Figs. 2 and 3 show the curves based on the data in Tab. 2. Namely, the dependence of the temperature changes of the steady state Ts on the frequency and stress in the activation zone.

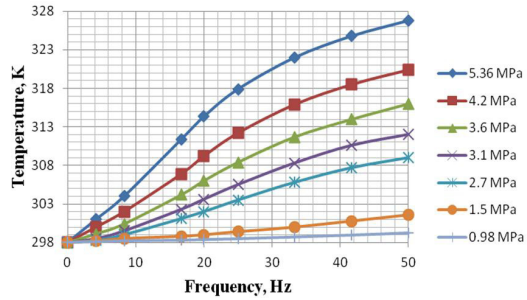

Fig. 2: Dependence of the steady state temperature of the activation zone Ts on the frequency of the cyclic load f, Hz at various maximum internal stress.

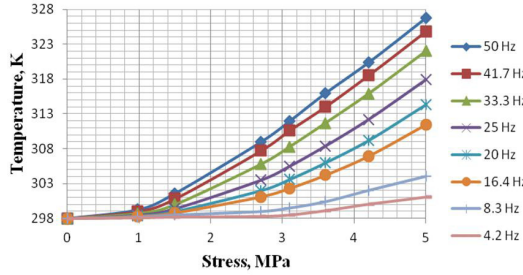

Fig. 3: Dependence of the steady state temperature of the activation zone Ts on the frequency of the cyclic load f, Hz at different maximum internal stress.

The typical character of the temperature *Ts* of the stationary state as a function of the frequency, according to the in-situ experiment and the results of computer calculations, changing in the range of 0 – 50 Hz at a stress of Yo = 3.6 MPa, model TEO (Eq. 9) is presented in Fig. 4.

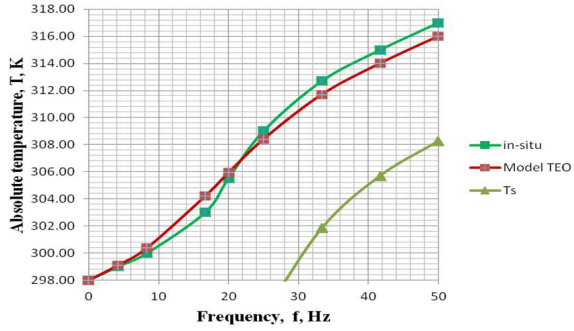

Fig. 4: Dependence of the steady-state temperature of the activation zone Ts on the frequency of the cyclic load f, Hz at a stress of M = 3.6 MPa.

Tab. 2: The experimental factor levels and test results.

Test serial number	Test group number	Test conditions		Test results	
		Variable factors		Temperature in stationary state, Ts, (K)	
		Console length, (mm) Max stress, (MPa)	Frequence (Hz)	Experiment in situ	Model TEO
1	1a	220 (5.36)	50.0	326.8b	328.7
	2		41.7	325.8	324.8
	3		33.3	324.0	322.0
	4		25.0	317.4	317.9
	5		20.0	315.2	314.4
	6		16.7	312.7	311.4
	7		8.3	305.7	304.0
	8		4.2	300.7	301.0
2	1	240 (4.2)	50.0	320.0	320.4
	2		41.7	319.7	318.5
	3		33.3	315.9	315.9
	4		25.0	313.5	312.2
	5		20.0	311.0	309.2
	6		16.7	307.2	306.9
	7		8.3	303.4	302.0
	8		4.2	300.9	300.0
3	1	260 (3.6)	50.0	317.0	316.2
	2		41.7	315.0	314.3
	3		33.3	312.7	311.7
	4		25.0	309.0	308.4
	5		20.0	305.5	305.9
	6		16.7	303.0	304.2
	7		8.3	300.0	300.4
	8		4.2	299.0	299.1
4	1	280 (3.1)	50.0	313.1	312.0
	2		41.7	311.6	310.6
	3		33.3	308.9	308.3
	4		25.0	305.6	305.5
	5		20.0	304.1	303.6
	6		16.7	304.3	302.3
	7		8.3	298.9	299.5
	8		4.2	299.6	298.5
5	1	300 (2.7)	50	309.0	308.0
	2		41.7	308.7	307.7
	3		33.3	307.8	305.8
	4		25	303.0	303.5
	5		20	302.8	302.0
	6		16.7	302.4	301.1
	7		8.3	300.7	299.0
	8		4.2	298.0	298.3
6	1	400 (1.52)	50	301.2	301.6
	2		41.7	302.0	300.8
	3		33.3	300.0	300.0
	4		25	300.7	299.4
	5		20	300.8	299.0
	6		16.7	299.1	298.8
	7		8.3	299.9	298.5
	8		4.2	299.1	298.2
7	1	500 (0.98)	50	300.7	299.3
	2		41.7	300.4	299.0
	3		33.3	299.9	298.7
	4		25	300.0	298.5
	5		20	298.7	298.4
	6		16.7	299.4	298.3
	7		8.3	300.3	298.2
	8		4.2	300.1	298.1

[a] 6 samples were used in each group.

[b] The confidence interval is indicated at p = 0.05 level.

The nature of the dependence of *Ts* on frequency *f* shows that the temperature graph has a characteristic S shape that exhibits a saturation property. At low frequencies of the cyclic load, the temperature grows slowly, however, as well as at high frequencies. The largest increase in the temperature of the stationary state occurs in the region of medium loading frequencies in the studied frequency range. All this suggests the presence and significant influence of internal friction in the material on the processes of internal deformation and its gradual destruction. It can be concluded that internal friction processes play a significant role in self-heating of this type of material. Examples of complete temperature change curves in the activation zone under cyclic loading of a rigid cantilever, close to failure, with the same cantilever length (the same power load) and different frequencies are shown in Fig. 5.

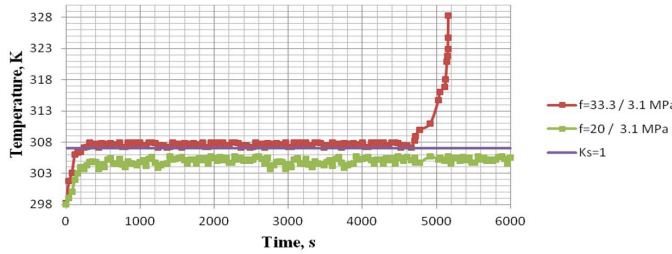

Fig. 5: Change in the temperature of the activation zone under cyclic loading of a rigid cantilever of the same size at different loading frequencies: f = 20 Hz and f = 33.3 Hz and the same load Yo = 3.1 MPa.

The results in Fig. 5 show that at a loading frequency f = 20 Hz, the steady state with the average temperature of the activation zone *Ts* = 303.6 K remained unchanged for almost an unlimited time. While at a frequency of *f* = 33.3 Hz, the stationary temperature *Ts* = 308.3 K was maintained for t_s = 4788 s and then increased. Intermediate current results, the temperature changes during the transition of the activation zone, first to the non-stationary state and then to the exacerbated mode and destruction, are shown in Fig. 6.

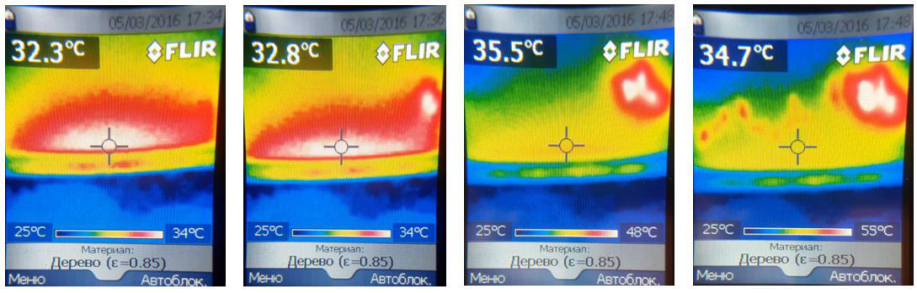

a) *b)* *c)* *d)*

Fig. 6: The thermograms of the surface of maximum stresses during of its cyclic loading; a) material in a stationary state; b) the thermogram 2 minutes after the end of the stationary state and the start of a non-stationary state; c) the thermogram 14 minutes after the start of the non-stationary state; d) the thermogram 14.5 minutes after the start of the non-stationary regime at the time of destruction.

The behaviour of the material in time qualitatively repeats the behaviour of the same material in a computational experiment. This is verified by the developed dynamic model for deformation and fracture of structurally heterogeneous materials such as particleboard.

Computational experiment

The aim of the computer experiment was to verify the adequacy of the behaviour of the dynamic model in the form of three differential equations (TEO model) to the behaviour of samples under cyclic loading. It is necessary to determine whether the model can describe the initial increase in temperature and its subsequent stabilization in the steady state. In order for the model to describe the specific conditions of the experiments, it must have initial and boundary conditions that are identical to the conditions for conducting a full-scale experiment. In this case, the initial and boundary conditions were the following dependencies:

$$\sigma\Big|_{t=0} = \sigma_0; T\Big|_{t=0} = T_0; \varepsilon\Big|_{t=0} = \varepsilon_0; x\Big|_{t=0} = x_0; Y\Big|_{t=0} = Y_0; \frac{d\sigma}{dt}\Big|_{t=0} = 0; \frac{dT}{dt}\Big|_{t=0} = 0;$$

$$\frac{d\varepsilon}{dt}\Big|_{t=0} = 0; \frac{dx}{dt}\Big|_{t=0} = 0; \frac{dY}{dt}\Big|_{t=0} = 0; \sigma_0 = 0; \varepsilon_0 = 0; T_0 = 298K$$

The boundary test conditions that are the magnitude of the loading parameters of the system were presented in Tab. 2. Remaining boundary conditions are presented in Tab. 1 in the form of constant values. The solution will be thought by the Runge-Kutta fourth order computational method in the internal time mode, which coincides with the real one.

The results of computer experiments are presented in Tab. 2. Fig. 7 shows a graph of the change in the average temperature of the activation zone in time under the boundary conditions: f = 50 Hz, Yo = 3.6 MPa. Under other boundary conditions, the nature of the curve does not change, but only the value of the maximum temperature is reached. The graph shows that the temperature from the initial temperature, T_o = 298 K, gradually rises and stabilizes at T_s = 315.85 K. All other values of stationary temperatures, depending on the boundary conditions, are presented in Tab. 2.

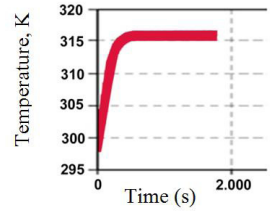

Fig. 7: Change in average temperature at f = 50 Hz and M = 3.6 MPa.

Fig. 8 shows graphs of changes in all three phase variables in the steady state. It can be seen that each of the variables is not a constant value, but fluctuates around its mean value. For example, the temperature varies from 315.55 to 316.14 K; internal stress from 6 to 4 MPa; deformation from -0,002 to + 0,002. Since over time, the boundaries of phase variables do not change, which means our dynamic system is in the region of a stable cycle – an attractor.

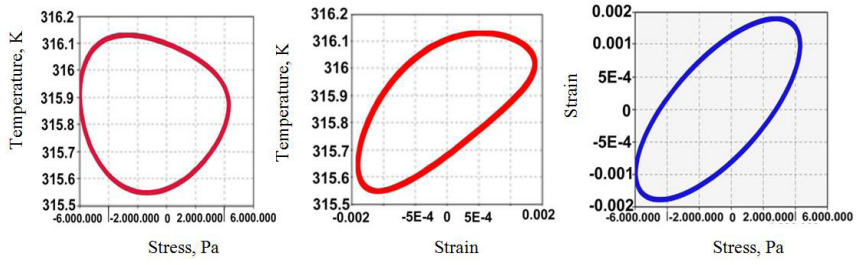

a) *b)* *c)*

Fig. 8: The nature of the phase trajectories changes in the stationary state of the system: a) temperature change Ts depending on changes in internal stresses, σ; b) temperature change Ts depending on the change in deformations, ε; c) stress variations σ due to deformations ε.

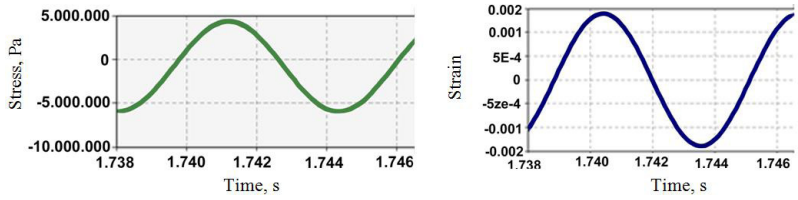

a) *b)*

Fig. 9: The nature of the changes of phase variables in the stationary state of the system: a) the change in internal stresses, σ; b) change of deformations, ε.

Based on obtained results, the stationarity criterion was determined by formula (13) for each group of experiments. The results are presented in Fig. 10.

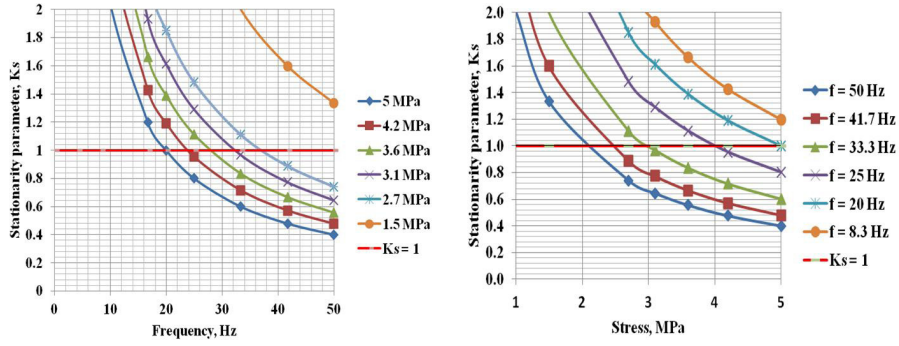

a) *b)*

Fig. 10: Change in the stationarity parameter Ks depending on: a) frequency, b) stress.

The data shown in Fig. 10 allow to distinguish two regions that differ in the magnitude of the stationarity parameter and, therefore, the nature of the system's behaviour when a steady state is reached. The lower region of the diagram in which *Ks* <1 is the region in the general case of the asymptotically unstable state of the system. That states where the probability of a system

transitioning to a non-stationary state is much higher than when Ks = 1. For example, for mode f = 33.1 Hz and M = 3.1 MPa in the diagram in Fig. 10a, the stationarity parameter Ks (33.1/3.1) = 0.89 lies below the line Ks = 1. The evolution of the system with this mode is shown in Fig. 5 (f = 33.1/3.1). After a certain time, the system went into a non-stationary state and then collapsed. The system loaded in accordance with the mode f = 20/3.1 has the stationarity parameter Ks (20/3.1) = 14.8 > Ks = 1, that is more stationary criterion. In this case, the system may be in a stationary state for an unlimited time.

In the initial period, when the inflow of external energy into the system is greater than its outflow from the system, the temperature gradually rises. With increasing temperature, its gradient increases and, consequently, the heat transfer of the system increases. At a certain point, the inflow and outflow of energy are equalized. After that, the temperature fluctuates with a small amplitude around its average value. However, if the temperature stabilizes and, at the same time, the outflow of energy from the system is less than a certain value, then this steady state will not be stable (or asymptotically stable) and after some time the system will move to a non-stationary state (see curve f = 33.3/3.1 MPa, Fig. 5). If the temperature stabilizes and, at the same time, the outflow of thermal energy from the system is less than a certain value, then such a stationary steady state cannot be considered as stable. This part of the external energy will dissipate within the system. Thus, the system should have a limiting stationary state, exceeding which the system will increase the probability of a transition to a non-stationary state and then to an exacerbated regime. The limit stationary state depends on the system itself and on the conditions of its loading.

At this stage, based on the comparison of results of computer experiments can be determined whether the system has exceeded the limiting steady state or not. Depending on this, it evaluates some of the risks of its future behaviour. Thus, the TEO model can be used as a basic forecasting model, since it adequately describes the initial moment of the system evolution and its transition to a stationary state.

CONCLUSIONS

Under the influence of an external cyclic load, the temperature in the activation zone of a polymer composite material gradually increases to a certain value and then stabilizes. This suggests that an open system gradually moves from an equilibrium state to a stationary state, which is characterized by an average temperature Ts. The nature of the dependence of Ts on frequency shows that the temperature graph has a characteristic S shape, which exhibits a saturation property. At low frequencies of the cyclic load, the temperature grows slowly, however, as well as at high frequencies. The largest increase in the temperature of the stationary state occurs in the region of medium loading frequencies in the studied frequency range. All this suggests the presence and significant influence of internal friction in the material on the processes of internal deformation and its gradual destruction. It can be concluded that this type of material internal friction processes plays a significant role in its self-heating.

A stationary criterion of the system was proposed, which allows determining the stability level of the stationary state of the system for each loading mode and each material.

In parallel with the full-scale experiment, a computational experiment was conducted on the proposed mathematical model in the form of a non-adiabatic thermoelastic oscillator. The results of the computational experiment confirmed mathematical description of the deformation process - the destruction of polymer composites in the form of a system of nonlinear differential

equations of the first order. The analysis of results of in-situ experiment and the computational experiment made it possible to formulate the concept of a critical exponent (order parameter) for fatigue failure. The behaviour of such dynamic system is completely determined by the magnitude of the order parameter. The critical value of the order parameter depends on the thermo-physical properties of the material and is equal to the ratio of the value of the heat transfer coefficient multiplied by the area of thermal dispersion to the coefficient of linear thermal expansion.

It is shown that the model of a non-adiabatic thermoelastic oscillator in the form of a system of three differential equations in partial derivatives can be used as a basic nonlinear dynamic model of the behaviour of such complex systems as structurally inhomogeneous media. The behaviour of these materials is adequately described by a dynamic system of differential equations, which includes three variables, namely, stress, strain, and temperature.

ACKNOWLEDGEMENT

This work was supported by the Slovak Research and Development Agency under contracts No. APVV-14-0506, APVV-17-0583 and APVV-18-0378.

REFERENCES

1. ASTM D 1037-12, 2012: Standard test methods for evaluating properties of wood-base fiber and particle panel materials.
2. Boiko, L.M., Grabar, I.G., Kulman, S.N., 2013: Durability of particleboards in furniture. Osvita Ukrainy, Ukraine, 210 pp.
3. Deliiski, N., Dzurenda, L., Angelski, D., Tumbarkova, N., 2019: Computing the energy for warming up the prisms for veneer production during autoclave steaming with a limited power of the heat generator. Acta Facultatis Xylologiae Zvolen 61(1): 63-74.
4. Dulieu-Barton, J.M., Stanley, P., 1999: Applications of thermoelastic stress analysis to composite materials. Strain 35(2): 41-48.
5. Emery, T.R., Dulieu-Barton, J.M., 2010: Thermoelastic stress analysis of damage mechanisms in composite materials. Composites Part A: Applied Science and Manufacturing 41(12): 1729-1742.
6. EN 312, 2010: Particleboards. Specifications, Brussels.
7. EN 13501-1, 2019: Fire classification of construction products and building elements. Part 1: Classification using data from reaction to fire tests. European Committee for Standardisation, Brussels.
8. Fruehmann, R.K., Dulieu-Barton, J.M., Quinn, S., 2010: Assessment of fatigue damage evolution in woven composite materials using infra-red techniques. Composites Science and Technology 70(6): 937-946.
9. Haken, H., 1983: Synergetics. An Introduction: Nonequilibrium Phase Transitions and Self-Organization in Physics, Chemistry, and Biology. Springer-Verlag. New York, 371 pp.
10. Ihnát, V., Lübke, H., Russ, A., Borůvka, V., 2017: Waste agglomerated wood materials as a secondary raw material for chipboards and fibreboards Part I. Preparation and characterization of wood chips in terms of their reuse. Wood Research 62(1): 45-56.
11. Iždinský, J., Reinprecht, L., 2017: Particleboards prepared with addition of copper sulphate. Part 2: Moisture and strength properties. Acta Facultatis Xylologiae Zvolen 59(2): 61-66.

12. Jones, R., Molent, L., 2004: Application of constitutive modelling and advanced repair technology to F111C aircraft. Composite Structures 66(1-4): 145-157.
13. Katunin, A., 2017: Domination of self-heating effect during fatigue of polymeric composites. Procedia Structural Integrity 5: 93-98.
14. Kulman, S.N., 2014: Predicting the durability of composite materials based on wood. Annals of Warsaw University of Life Sciences 86: 175-179.
15. Kulman, S.N., 2015: Method of non-destructive control and prediction of durability of details of wood and wood materials during their cyclic loading. UA Patent 100386.
16. Kulman, S., Boiko, L., 2016: Non-linear effects in the reaction of wood composite materials during the thermal, humidity and power loads. Annals of Warsaw University of Life Sciences 95: 159-165.
17. Kulman, S., Boiko, L., Pinchevska, O., Sedliačik, J., 2017: Durability of wood-based panels predicted using bending strength results from accelerated treatments. Acta Facultatis Xylologiae Zvolen 59(2): 41-52.
18. Kúdela, J., 2017: Moisture-content-related stability of beech plywood and particleboard beams loaded in buckling. Acta Facultatis Xylologiae Zvolen 59(2): 33-40.
19. Landau, L.D., Lifshitz, E.M., 1986: Theory of elasticity. Butterworth-Heinemann. London, 248 pp.
20. Lin, S.T., Rowlands, R.E., 1995: Thermoelastic stress analysis of orthotropic composites. Experimental Mechanics 35(3): 257-265.
21. Naderi, M., Khonsari, M.M., 2012: Thermodynamic analysis of fatigue failure in a composite laminate. Mechanics of Materials 46: 113-122.
22. Novák, I., Pavlinec, J., Chodák, I., Preťo, J., Vanko, V., 2018: Metallocene polyolefins for hot-melt adhesive preparation. Annals of Warsaw University of Life Sciences – SGGW Forestry and Wood Technology 104: 154-157.
23. Palumbo, D., De Finis, R., Demelio, G.P., Galietti, U., 2017: Study of damage evolution in composite materials based on the Thermoelastic Phase Analysis (TPA) method. Composites Part B: Engineering 117: 49-60.
24. Pavlinec, J., Novák, I., Rychlý, J., Kleinová, A., Nógellová, Z., Preťo, J., Vanko, V., Žigo, O., Chodák, I., 2018: Hot melt adhesives prepared by grafting of acrylic and crotonic acids onto metallocene ethylene-octene copolymers. Journal of Plastic Film and Sheeting, 1-21.
25. Paynter, R.J.H., Dutton, A.G., 2003: The use of a second harmonic correlation to detect damage in composite structures using thermoelastic stress measurements. Strain 39(2): 73-78.
26. Sfarra, S., Perilli, S., Ambrosini, D., Paoletti, D., Nardi, I., de Rubeis, T., Santulli, C., 2017. A proposal of a new material for greenhouses on the basis of numerical, optical, thermal and mechanical approaches. Construction and Building Materials 155: 332-347.
27. Thomson, W., 1853: On the dynamical theory of heat. Earth and Environmental Science Transactions of the Royal Society of Edinburgh 2013, 20(2): 261-283.
28. Toubal, L., Karama, M., Lorrain, B., 2006: Damage evolution and infrared thermography in woven composite laminates under fatigue loading. International Journal of Fatigue 28: 1867-1872.
29. Uenoya, T., Fujii, T., 2000: Nondestructive damage characterization of carbon fiber composites through improved thermoelastic technique. Journal of the Society of Materials Science, Japan 49(8): 941-947.

30. Yoshida, T., Uenoya, T., Miyamoto, H., 2012: Impact damage characterization in cross-plied carbon fiber/thermoplastic composites using thermoelastic stress analysis. Proceedings of SPIE, 8 pp.

Sergiy Kulman, Liugmyla Boiko
Zhytomyr National Agroecological University
Faculty of Forestry
Department of Wood Processing
Zhytomyr
Ukraine

Diana Hamáry Gurová, *Ján Sedliačik
Technical University in Zvolen,
Faculty of Wood Sciences and Technology
Department of Furniture and Wood Products
Zvolen
Slovak Republic
*Corresponding author: sedliacik@tuzvo.sk